Catal Lett (2009) 129:250–257
DOI 10.1007/s10562-008-9810-0

Characterization and Catalytic Properties of the Ni/Al_2O_3 Catalysts for Aqueous-phase Reforming of Glucose

Guodong Wen · Yunpeng Xu · Zhusheng Xu · Zhijian Tian

Received: 2 November 2008 / Accepted: 29 November 2008 / Published online: 13 December 2008

Abstract Two Ni/Al_2O_3 catalysts with high Ni loadings of 36 wt% and 48 wt%, which possess high activities for aqueous-phase reforming of glucose, have been successfully prepared by a novel two-step impregnation method. The catalytic performance was investigated at 533 K and autogenous pressure in a batch reactor and a significant enhancement in hydrogen yield was observed over the catalyst prepared by two-step impregnation as compared to the corresponding catalyst prepared by conventional single impregnation. The catalysts were characterized by XRD, N_2 adsorption/desorption, H_2 chemisorption, O_2 uptake, TPO, H_2-TPR and TEM. It was found that two-step impregnation yielded catalysts with higher nickel dispersion as well as smaller nickel particle size compared to single impregnation.

Keywords Aqueous-phase reforming · Glucose · Hydrogen · Ni/Al_2O_3

G. Wen · Y. Xu · Z. Xu · Z. Tian (✉)
Laboratory of Applied Catalysis, Dalian Institute of Chemical Physics, Chinese Academy of Sciences, 457 Zhongshan Road, Dalian 116023, People's Republic of China
e-mail: tianz@dicp.ac.cn

G. Wen
Graduate University of Chinese Academy of Sciences, 19 Yuquan Road, Beijing 100049, People's Republic of China

Z. Tian
State Key Laboratory of Catalysis, Dalian Institute of Chemical Physics, Chinese Academy of Sciences, 457 Zhongshan Road, Dalian 116023, People's Republic of China

1 Introduction

Biomass was considered as a promising renewable source for hydrogen production compared to the diminishing fossil fuels [1]. Recently, a new process has been reported by Dumesic and co-workers that hydrogen could be efficiently produced from biomass-derived glucose and polyols at mild conditions near 500 K in a single fixed-bed flow reactor aqueous-phase reforming (APR) process [2]. This process is energy saving because part of the water and the oxygenated hydrocarbons with low volatility were not allowed to vaporize. Moreover, APR occurs at low temperatures that the water–gas shift (WGS) reaction is thermodynamically favored, thus lead to low levels of CO.

Particular attention had been paid to glucose [3–6], the only compound in this class of reactants that is directly relevant to biomass utilization. APR of glucose occurs according to the following stoichiometric reaction [7]:

$$C_6H_{12}O_6 + 6H_2O \rightarrow 12H_2 + 6CO_2 \quad (1)$$

The following two main reactions would occur during the reaction conditions:

$$C_6H_{12}O_6 \rightarrow 6H_2 + 6CO \quad (2)$$

$$CO + H_2O \rightarrow CO_2 + H_2 \quad (3)$$

Pt catalysts were identified as promising catalysts for the APR reactions [7]. However, the high cost of Pt makes it advantageous to develop non-precious catalysts. Although non-precious Ni catalyst showed high initial activity that was comparable to Pt catalyst, significant deactivation was observed [8]. Efforts have been made to improve the catalytic activities of the Ni catalysts by impregnating another metal components [9, 10]. Furthermore, modified skeletal Ni catalysts were developed to improve the

stability of the aforementioned bimetallic catalysts [11, 12]. In the present study, a novel two-step impregnation technique for the preparation of the Ni/Al_2O_3 catalysts was developed, and the catalysts were tested in the APR of glucose. It was noteworthy that the catalysts with high Ni loadings prepared by two-step impregnation exhibited significantly superior catalytic properties than the corresponding catalysts prepared by conventional single impregnation.

2 Experimental

2.1 Catalyst Preparation

The catalysts were prepared by impregnation Al_2O_3 with a solution containing the required amount of $Ni(NO_3)_2{\cdot}6H_2O$. After impregnating with Ni, the samples were evaporated at 353 K to dryness, then dried at 383 K overnight, and finally calcined in air at 723 K for 3 h. The Al_2O_3 used was derived from pseudo-boehmite. It has been calcined in air at 773 K for 3 h prior to impregnation. Two groups of Ni catalysts were prepared according to the following detailed steps.

1. *Single impregnation*. The calcined as-prepared samples with different Ni loadings of 14 wt%, 21 wt%, 27 wt%, 36 wt%, and 48 wt% were denoted as 14 wt% Ni/Al_2O_3(S), 21 wt% Ni/Al_2O_3(S), 27 wt% Ni/Al_2O_3(S), 36 wt% Ni/Al_2O_3(S), and 48 wt% Ni/Al_2O_3(S), respectively.
2. *Two-step impregnation*. In the case of two-step impregnation, the first impregnation was carried out by impregnation, evaporation, drying and calcination, and then the same operation with the same additive amount of Ni was repeated. The calcined as-prepared catalysts with Ni loadings of 27 wt%, 36 wt%, and 48 wt% were denoted as 27 wt% Ni/Al_2O_3(T), 36 wt% Ni/Al_2O_3(T), and 48 wt% Ni/Al_2O_3(T), respectively.

Prior to catalyst ex situ studies such as XRD, N_2 adsorption/desorption, and TEM, all of the Ni/Al_2O_3 catalysts were reduced in flowing H_2 for 2 h at 823 K, then cooled to room temperature and passivated in a stream of O_2/N_2 (1% O_2).

2.2 Catalyst Characterization

The chemical compositions (Ni loadings) of the samples were determined with a Philips Magix601 X-ray fluorescence (XRF) analysis apparatus. Powder XRD patterns of the catalysts were recorded on a PANalytical X'Pert PRO diffractometer using Cu K_α radiation ($\lambda = 1.5404$ Å) at 40 kV and 40 mA. A NOVA-4000 physical adsorption instrument was used to measure the N_2 adsorption–desorption isotherms of the samples at 77 K. The specific surface area was determined from the linear portion of the BET plot. The pore-size distribution was calculated from the desorption isotherm using the Barrett–Joyner–Halenda (BJH) formula. Prior to the measurements, the samples were degassed in vacuum at 623 K for 2 h to remove physically adsorbed components. Transmission electron microscopy (TEM) measurements were carried out on a FEI Tecnai G^2 microscope. The samples were ultrasonically suspended in ethanol and placed onto a copper grid.

H_2 pulse chemisorption was measured at room temperature in a homemade setup with a TCD detector. A catalyst sample of 100 mg was reduced in H_2 flow at 823 K for 2 h. After reduction, the temperature was kept in a Ar flow at 823 K for 2 h and thereafter allowed to cool to room temperature for in situ chemisorption measurement. The exposed Ni atoms were assumed as H/Ni atomic ratio of 1:1. The oxygen pulse uptake was measured at 723 K with 4.5% O_2/Ar. The amount of oxygen consumed was detected using an online mass spectrometry (OminiStar GSD 300, Balzers).

Temperature-programmed reductions (TPR) of catalysts were conducted with 5% H_2/Ar mixed gas at a flow rate of 37 mL/min (STP) from 303 to 1,073 K at a constant heating rate (10 K/min). Temperature-programmed oxidation (TPO) of catalyst was conducted with 4.5% O_2/Ar mixed gas at a flow rate of 37 mL/min (STP) from 303 to 1,073 K at a constant heating rate (10 K/min). The gas effluent was monitored online with a mass spectrometry mentioned above.

2.3 Catalytic Activity Test

The APR of glucose was performed in a homemade batch reactor described elsewhere [5]. The reaction was carried out under autogenous pressure with continuous magnetic stirring. In a typical experiment, 1.0 g catalyst, 90 g H_2O and the required amount of $C_6H_{12}O_6{\cdot}H_2O$ were put inside the reactor. The reactor was thoroughly purged with argon, and then heated to the desired temperature at a certain heating rate. The reaction time started after reaching the desired temperature. When the reaction finished, the reaction was quenched by cold water. The quantity of the gas product was measured after the reaction by wet gas flowmeter. Prior to the activity test, the Ni catalysts were reduced for 2 h at 823 K and ambient pressure with a heating rate of 2 K/min.

The gas products were analyzed according to the method described elsewhere [13]. The liquid product was drained after reaction, and then analyzed by inductively coupled plasma atomic emission spectrometry (ICP-AES), gas chromatography-mass spectroscopy (GC6890-MS5973 N,

Agilent) with a HP-Innowax capillary column, HPLC (Elite, RI detector, Sugar SC-1011 column (Shodex)) and total organic carbon (TOC).

3 Results and Discussion

3.1 Physicochemical Characterization

3.1.1 BET Surface Area and Pore Structure

Table 1 showed the physical properties of support and Ni/Al_2O_3 catalysts. All samples exhibited type IV isotherms typical of a mesoporous texture. As the Ni loadings of the Ni/Al_2O_3 catalysts prepared by single impregnations increased from 14 to 48 wt%, the surface area (S_{BET}) and the pore volume (V_p) gradually decreased, which suggested a negative effect of Ni on texture properties. However, the pore diameter of the catalysts did not change significantly. Moreover, 36 wt% Ni/Al_2O_3(T) and 48 wt% Ni/Al_2O_3(T) showed smaller surface area and pore volume than 36 wt% Ni/Al_2O_3(S) and 48 wt% Ni/Al_2O_3(S), respectively, whereas 27 wt% Ni/Al_2O_3(T) exhibited larger surface area and pore volume than 27 wt% Ni/Al_2O_3(S).

3.1.2 X-ray Diffraction (XRD)

Figure 1 showed the XRD patterns of the samples calcined at 723 K for 3 h, and the characteristic peaks of NiO were marked in the figure. As expected, the characteristic peaks of NiO were gradually intensified, and their peak width at half height lessened as the Ni content increased for the catalysts prepared by single impregnations. The results indicated that the amount of detectable crystalline NiO and the particle size of NiO increased with increasing of the Ni content. It can be also seen from the figure that the characteristic peaks of NiO for 27 wt% Ni/Al_2O_3(T), 36 wt% Ni/Al_2O_3(T) and 48 wt% Ni/Al_2O_3(T) samples were weaker and broader than those for 27 wt% Ni/Al_2O_3(S), 36 wt% Ni/Al_2O_3(S) and 48 wt% Ni/Al_2O_3(S) samples, respectively. The results suggested that the calcined Ni/Al_2O_3 catalysts prepared by two-step impregnations had smaller amount of detectable crystalline NiO as well as smaller NiO particle size than the corresponding catalysts prepared by single impregnations. In addition, three broad peaks at $2\theta = 37.5°$, 46°, and 67° in the XRD curve of bare alumina indicated the presence of amorphous γ-Al_2O_3.

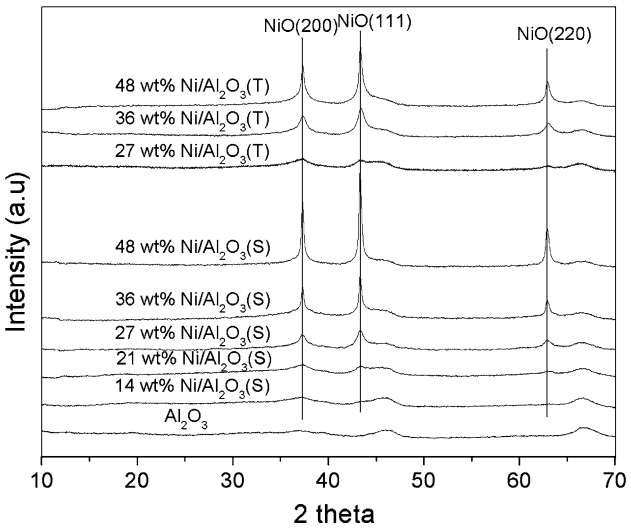

Fig. 1 Powder XRD spectra of Ni/Al_2O_3 samples calcined at 723 K for 3 h

Table 1 Physical properties of support and Ni/Al_2O_3 catalysts

Catalysts	S_{BET} (m^2/g)	V_p (cm^3/g)[a]	D_p (nm)[b]
Al_2O_3	249.7	0.54	6.60
14 wt% Ni/Al_2O_3(S)	195.7	0.45	6.56
21 wt% Ni/Al_2O_3(S)	187.9	0.41	6.53
27 wt% Ni/Al_2O_3(S)	181.0	0.38	6.59
36 wt% Ni/Al_2O_3(S)	159.3	0.31	6.52
48 wt% Ni/Al_2O_3(S)	124.4	0.27	6.62
27 wt% Ni/Al_2O_3(T)	184.1	0.45	6.57
36 wt% Ni/Al_2O_3(T)	138.3	0.30	6.56
48 wt% Ni/Al_2O_3(T)	116.2	0.25	6.57

[a] Pore volume is calculated from the desorption branch of physisorption isotherm

[b] BJH desorption average pore diameter

The XRD patterns of reduced Ni/Al_2O_3 catalysts were shown in Fig. 2. Decreasing Ni content in the catalysts prepared by single impregnations resulted in broader and weaker characteristic peaks of Ni^0. In addition, the characteristic peaks of Ni^0 for 27 wt% Ni/Al_2O_3(T), 36 wt% Ni/Al_2O_3(T) and 48 wt% Ni/Al_2O_3(T) samples were broader and weaker than those for 27 wt% Ni/Al_2O_3(S), 36 wt% Ni/Al_2O_3(S) and 48 wt% Ni/Al_2O_3(S), respectively. The results indicated that the amount of detectable crystalline Ni^0 and the particle size of metallic Ni increased with increasing of the Ni content for the catalysts prepared by single impregnations, while the catalysts prepared by two-step impregnations had smaller amount of detectable crystalline Ni^0 and metallic Ni particle size than the corresponding catalysts prepared by single impregnations. Furthermore, the NiO and metallic Ni particle size were calculated by Scherre equation from NiO(200) and Ni(111) planes, respectively, the results agreed well with the above deduction.

3.1.3 Transmission Electron Microscopy (TEM)

The micrographs of reduced 36 wt% Ni/Al_2O_3 and 48 wt% Ni/Al_2O_3 catalysts prepared by single and two-step

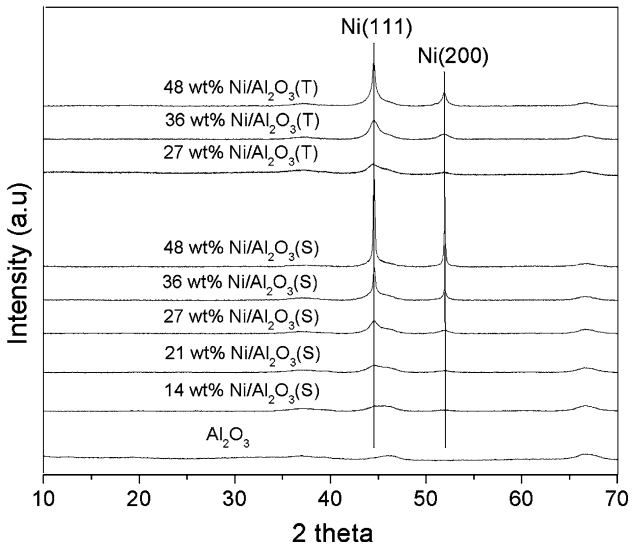

Fig. 2 Powder XRD spectra of Ni/Al_2O_3 samples reduced at 823 K for 2 h

impregnations are shown in Fig. 3. It can be seen from the figures that Ni particles were irregularly dispersed on platelet-like Al_2O_3 support. In addition, the 36 wt% Ni/Al_2O_3(S) and 48 wt% Ni/Al_2O_3(S) were found to yield larger Ni particle size compared to 36 wt% Ni/Al_2O_3(T) and 48 wt% Ni/Al_2O_3(T), respectively. The above results from TEM are in accordance with the results from XRD.

3.1.4 H_2 Temperature Programmed Reduction (H_2-TPR)

The H_2-TPR curve of calcined Ni/Al_2O_3 samples was shown in Fig. 4. Figure 4a exhibited the TPR patterns of Ni/Al_2O_3 catalysts prepared by single impregnations. For the 27 wt% Ni/Al_2O_3(S) sample, three peaks were observed: a high temperature peak at ca. 1,060 K and two low temperature peaks at ca. 545 K and ca. 800 K, respectively. The two low temperature peaks were attributed to reduction of NiO with weaker interaction with Al_2O_3 such as amorphous NiO and crystalline NiO, respectively, while the high temperature peak was attributed to reduction of $NiAl_2O_4$ [14, 15]. The three peaks were difficult to discern as the Ni loadings decreased from 27 to 14 wt%. When the Ni loadings increased from 27 to 48 wt%, the high temperature peak shifted towards lower temperature, indicating that higher metal content favored

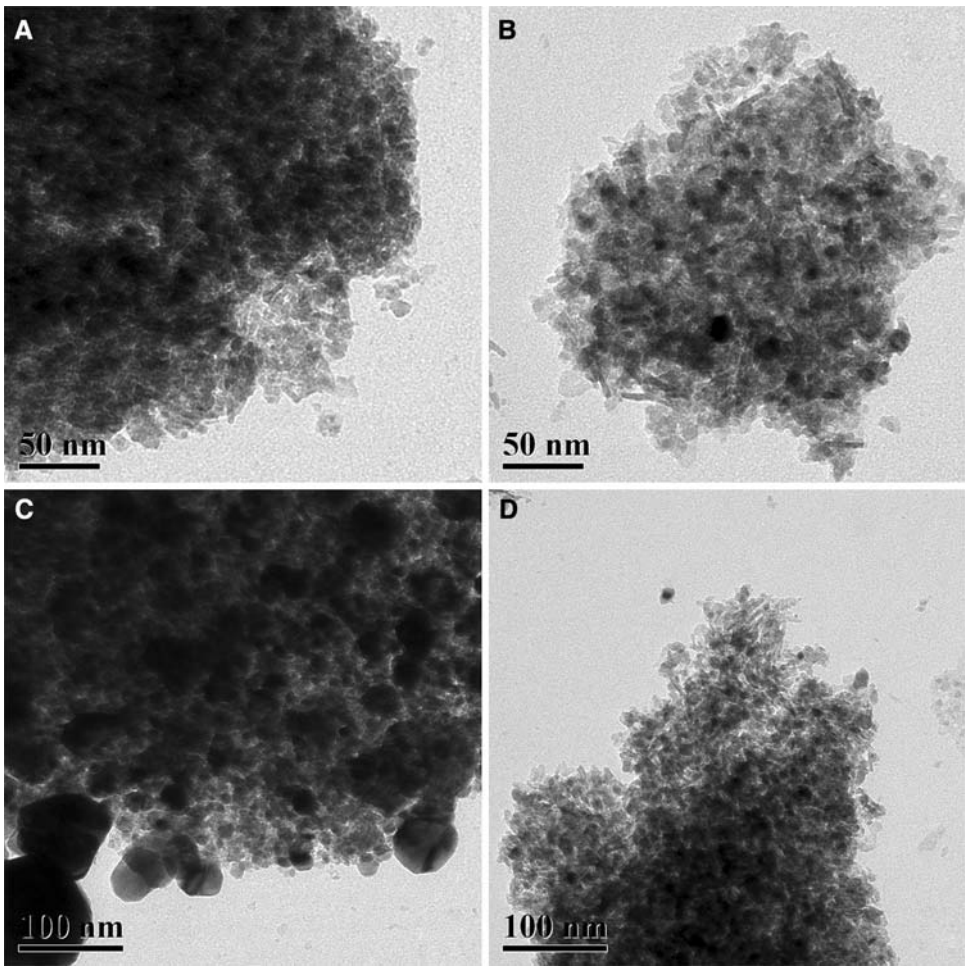

Fig. 3 TEM images of Ni/Al_2O_3 catalysts reduced at 823 K for 2 h. **a** 36 wt% Ni/Al_2O_3(S), **b** 36 wt% Ni/Al_2O_3(T), **c** 48 wt% Ni/Al_2O_3(S), and **d** 48 wt% Ni/Al_2O_3(T)

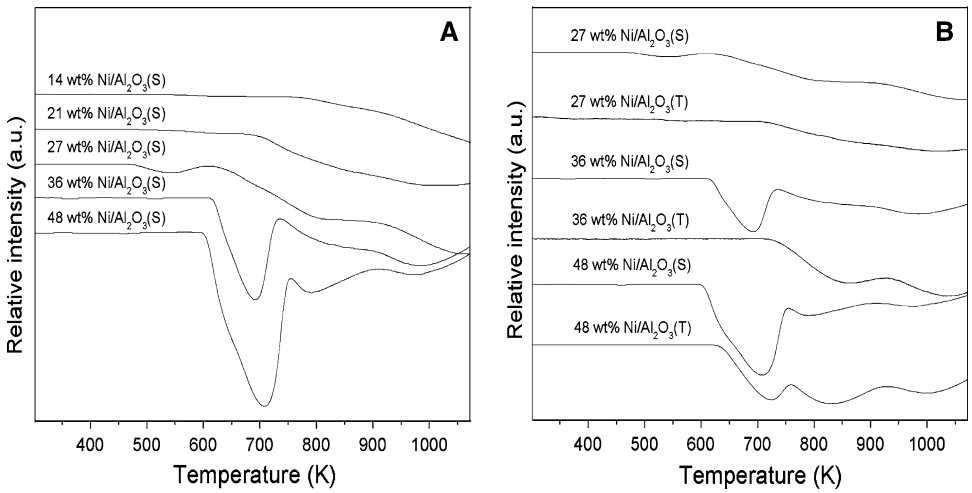

Fig. 4 H_2-TPR curves of Ni/Al_2O_3 samples calcined at 723 K for 3 h. **a** Catalysts prepared by single impregnation with Ni loadings ranging from 14 to 48 wt%. **b** 27 wt% Ni/Al_2O_3, 36 wt% Ni/Al_2O_3 and 48 wt% Ni/Al_2O_3 catalysts prepared by single impregnations and two-step impregnations

the formation of more readily reducible Ni species [16, 17]. Moreover, a low temperature peak at ca. 700 K with high intensity was observed, whereas the low temperature peak at ca. 545 K severely attenuated. The results indicated that large amount of crystalline NiO was formed, whereas the amount of amorphous NiO remarkably decreased. Figure 4b compared the H_2-TPR profiles of 27 wt% Ni/Al_2O_3, 36 wt% Ni/Al_2O_3 and 48 wt% Ni/Al_2O_3 catalysts prepared by single impregnations and two-step impregnations. For the 27 wt% Ni/Al_2O_3 samples, only one high temperature peak at ca. 1,020 K was observed on 27 wt% Ni/Al_2O_3(T), whereas two additional lower temperature peaks were found on 27 wt% Ni/Al_2O_3(S). For the 36 wt% Ni/Al_2O_3 samples, only two peaks at ca. 860 K and 1,040 K were shown on 36 wt% Ni/Al_2O_3(T), whereas a additional lower temperature peak at ca. 700 K was exhibited on 36 wt% Ni/Al_2O_3(S). For the 48 wt% Ni/Al_2O_3 samples, all of the three peaks which were similar to those for 36 wt% Ni/Al_2O_3(S) were displayed on both the 48 wt% Ni/Al_2O_3(S) and 48 wt% Ni/Al_2O_3(T) samples. However, the three peaks shifted towards slightly higher temperatures for the 48 wt% Ni/Al_2O_3(T) sample. The results indicated that the less reducible Ni species with strong interaction with the support were more prevalent in catalysts prepared by two-step impregnations, and was associated with the formation of smaller Ni particles as shown in Table 2.

3.1.5 H_2 Chemisorption and O_2 Uptake

Based on the assumption that unreduced NiO is present in a separate dispersed phase in intimate contact with the support, we calculated the Ni dispersion from the combination of the H_2 chemisorption and O_2 uptake data [18, 19]. As listed in Table 2, the Ni surface area exhibited a maximum at Ni loading of 27 wt% for the samples prepared by single impregnations. The 36 wt% Ni/Al_2O_3(T) and 48 wt% Ni/Al_2O_3(T) catalysts showed higher Ni surface area than 36 wt% Ni/Al_2O_3(S) and 48 wt% Ni/Al_2O_3(S), respectively, whereas 27 wt% Ni/Al_2O_3(T) exhibited lower Ni

Table 2 Results of H_2 chemisorption, O_2 uptake and XRD tests for Ni/Al_2O_3

Catalysts	Chemisorption[a]			XRD[b]	
	Ni surface area (SA_{Ni}, $m^2\ g_{cat}^{-1}$)	Reduction degree (f, %)	Ni dispersion (D_{Ni}, %)	d_{NiO} (nm)	d_{Ni} (nm)
14 wt% Ni/Al_2O_3(S)	4.0	24.6	17.2	–	2.9
21 wt% Ni/Al_2O_3(S)	10.3	48.4	15.4	5.0	3.0
27 wt% Ni/Al_2O_3(S)	11.4	39.6	16.2	11.0	6.9
36 wt% Ni/Al_2O_3(S)	9.3	45.3	8.0	28.7	26.3
48 wt% Ni/Al_2O_3(S)	7.9	51.8	4.7	30.0	38.5
27 wt% Ni/Al_2O_3(T)	6.5	18.3	20.1	5.6	4.0
36 wt% Ni/Al_2O_3(T)	11.9	41.1	12.1	12.4	7.4
48 wt% Ni/Al_2O_3(T)	13.4	53.5	7.8	24.3	20.0

[a] D_{Ni} (%) = 1.17X/(Wf), where X is the H_2 uptake from H_2 chemisorption, W is the weight percent of Ni in sample, f is the reduction degree obtained from O_2 uptake data and D_{Ni} is the Ni dispersion corrected for the amount reduced to metal [18, 19]

[b] d_{NiO} and d_{Ni} are from XRD data of NiO (200) and Ni (111) planes, respectively

surface area than 27 wt% Ni/Al_2O_3(S). Higher Ni dispersions were observed on 27 wt% Ni/Al_2O_3(T), 36 wt% Ni/Al_2O_3(T) and 48 wt% Ni/Al_2O_3(T) as compared to 27 wt% Ni/Al_2O_3(S), 36 wt% Ni/Al_2O_3(S) and 48 wt% Ni/Al_2O_3(S), respectively. The results indicated that two-step impregnations effectively promoted the dispersion of Ni compared to single impregnations.

3.2 Catalytic Activity

3.2.1 Effect of Ni Content and Impregnation Method on Catalytic Performance

Table 3 showed the results for the APR of glucose over the Ni/Al_2O_3 samples. It can be seen from the table that the hydrogen selectivities and yields increased gradually from Ni loadings ranging from 14 to 21 wt%, then greatly increased to 27 wt%, and finally showed slight increase in the range of 27–48 wt%. It can be also seen from the table that 36 wt% Ni/Al_2O_3(T) and 48 wt% Ni/Al_2O_3(T) gave higher conversion of C to gas, hydrogen yields and methane selectivities, as well as lower CO molar concentrations than 36 wt% Ni/Al_2O_3(S) and 48 wt% Ni/Al_2O_3(S), respectively, whereas 27 wt% Ni/Al_2O_3(T) exhibited lower hydrogen yield, hydrogen selectivity, and CO concentration than 27 wt% Ni/Al_2O_3(S).

It can be seen from Table 2 that the metallic Ni particle size of the samples prepared by single impregnations increased from 2.9 to 38.5 nm as the Ni loadings increased from 14 to 48 wt%, and the catalysts prepared by two-step impregnations exhibited smaller metallic Ni particle size than the corresponding catalysts prepared by single impregnations. Combing the results from Table 3, it can be found that high hydrogen selectivities were observed over catalysts with metallic Ni particle size larger than ca. 7 nm for the catalysts prepared by single impregnations. In a parallel, similar high hydrogen selectivities were observed over 36 wt% Ni/Al_2O_3(T) and 48 wt% Ni/Al_2O_3(T) with metallic Ni particle size larger than 7 nm, whereas low hydrogen selectivity was obtained on 27 wt% Ni/Al_2O_3(T) with smaller metallic Ni particle size. It was assumed that the catalytic properties of the catalysts were related to the metallic Ni particle size. It seems that the APR of glucose over these Ni catalysts is a structure sensitive process, analogous to the APR of glycerol on Pt/Al_2O_3 catalysts [20].

Although the conversion of glucose for 48 wt% Ni/Al_2O_3(T) reached nearly 95%, only 32.6% of carbon in the initial feed was converted into the gas products, indicating that large amount of carbon was either converted into the liquid phase or deposited on the catalyst. Propanal, acetone, 2-butanone, ethanol, 1-propanol, cyclopentanone, 1-pentanol, 3-pentanol, 2,5-hexanedione, 2,3-dimethyl-cyclopentenone, 5-ethyldihydro-2-furanone, and phenol were found by GC-MS in the liquid effluent. In addition, the carbon balance based on TOC analysis of the liquid product showed that 34.1% of carbon in the initial feed deposited on the catalyst. The carbon deposition was further identified by TPO characterization. In a parallel, it was

Table 3 Experimental results for the APR of 2.4 wt% glucose at 533 K and autogenous pressure over Ni/Al_2O_3 for 4 h

Catalysts	14 wt% Ni/Al_2O_3(S)	21 wt% Ni/Al_2O_3(S)	27 wt% Ni/Al_2O_3(S)	36 wt% Ni/Al_2O_3(S)	48 wt% Ni/Al_2O_3(S)	27 wt% Ni/Al_2O_3(T)	36 wt% Ni/Al_2O_3(T)	48 wt% Ni/Al_2O_3(T)	Blank[a]
Glucose conversion (%)	100	100	100	100	94.7	100	95.2	94.8	96.3
Conversion of C to gas (%)	7.6	7.8	12.6	13.1	16.5	12.6	33.3	32.6	6.0
Gas-phase composition									
H_2 (mol.%)	18.1	24.3	40.4	41.7	46.9	38.0	47.3	48.5	12.3
CO_2 (mol.%)	75.4	69.2	54.2	53.6	49.0	57.1	46.5	45.2	80.2
CO (mol.%)	4.9	5.0	4.0	3.3	2.3	3.4	0.3	0.3	7.0
CH_4 (mol.%)	0.2	0.5	1.0	0.9	1.4	0.9	5.3	5.4	0.1
C_2–C_6 hydrocarbons (mol.%)	1.5	0.9	0.5	0.5	0.4	0.6	0.6	0.5	0.4
H_2 selectivity (%)[b]	10.5	15.6	33.3	35.2	43.5	30.1	44.0	46.3	7.0
CH_4 selectivity (%)	0.2	0.7	1.6	1.5	2.6	1.4	9.9	10.4	0.2
Alkane selectivity (%)[c]	6.4	4.7	4.1	4.0	4.8	4.3	12.8	13.0	1.6
H_2 yield (%)[d]	0.8	1.2	4.2	4.6	7.2	3.8	14.7	15.1	0.4

[a] Experiment performed in the absence of metal catalyst

[b] H_2 selectivity (%) = (moles of H_2 produced/moles of C atoms in gas phase) × 2 × 100 [2]

[c] Alkane selectivity (%) = (moles of C in gaseous alkanes/total moles of C in gas phase) × 100 [2]

[d] Hydrogen yield is defined as the amount of hydrogen in the gaseous products normalized by the amount of hydrogen that would be present if the carbon atoms in the initial feed had all participated in the reforming reaction

found that part of the carbon was reversibly adsorbed on the catalyst and could be washed away by ethanol, which was consistent with the reference describe elsewhere [21]. The above results indicated that the side degradation reactions severely occurred during the APR of glucose [22]. However, it has been reported recently by Dumesic et al. that the degradation liquid products could be further efficiently converted to specific liquid fuels by integrating several flow reactors operated in a cascade mode [23].

3.2.2 *Effect of Residence Time on Catalytic Performance*

The effect of residence time on catalytic performance was shown in Fig. 5. It can be seen from the figure that the hydrogen selectivities exhibited a maximum at ca. 60 min. The molar concentrations of CO decreased with the increasing of the residence time within the considered residence time range. The hydrogen yields increased sharply in the residence time range of 2–60 min, then gradually increased to 360 min, and finally decreased slowly after 360 min.

It was reported that high concentrations of glucose lead to low hydrogen selectivities because of the homogeneous decomposition reactions [2], thus low hydrogen selectivity was observed at the initial stage of the reaction due to the high glucose initial concentration. In addition, it can be seen from Table 3 that the homogeneous degradation reactions lead to high CO concentration as shown in the blank experiment. Therefore, it can be deduced that the homogeneous degradation reactions were severely promoted at the initial stage of the reaction, thus lead to high CO concentration. It seems that the reforming reaction gradually dominated with the decrease of glucose concentrations in the residence time range of 60–240 min, thus lead to high hydrogen selectivities as well as low CO concentrations. However, the methanation reaction seems gradually to be dominant at longer residence time, thus lead to low hydrogen selectivity.

3.3 Catalytic Stability

To investigate the catalytic stability, the 48 wt% Ni/Al_2O_3(T) sample was used in repeated run. After the first run, the catalyst was separated by centrifugation and washed with ethanol and water, fresh glucose and water were added, and the mixture was used for the next run. However, the glucose conversion decreased to 75.2% after the first run. In addition, the hydrogen yield decreased to 7.2%, which was equivalent to only 47.7% of the yield for the fresh catalyst. The metallic Ni particle size of the spent catalyst from the XRD patterns increased to 23.8 nm compared to the metallic Ni particle size of 20.0 nm for the fresh catalyst, indicating that the Ni catalyst slightly sintered during the APR reaction conditions. The TPR profiles of the spent and fresh calcined 48 wt% Ni/Al_2O_3(T) were shown in Fig. 6. It can be seen from the figure that the spent catalyst took up hydrogen below 823 K at which temperature it was reduced. It can be also seen that the spent catalyst exhibited lower temperature peaks of H_2 consumption than the fresh calcined catalyst. The results indicated that the reduced catalyst were partly oxidized during APR reaction conditions, and the interaction between metal species and support was weakened during the APR reaction conditions. Moreover, inductively coupled plasma atomic emission spectrometry (ICP-AES) analysis of the liquid products showed a Ni effluent concentration of 38 wppm after the first run.

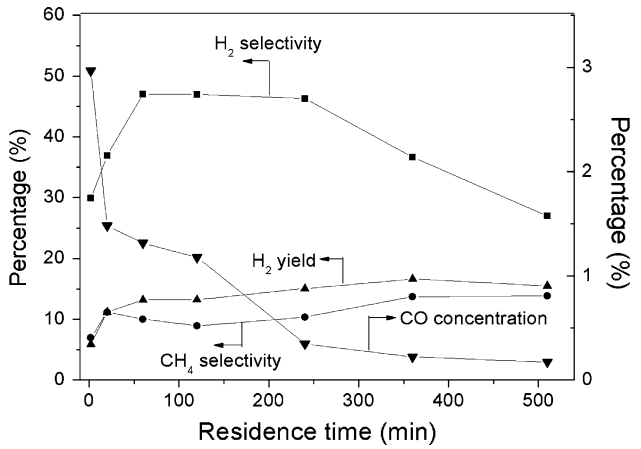

Fig. 5 Effect of residence time on the APR of 2.4 wt% glucose at 533 K and autogenous pressure over 48 wt% Ni/Al_2O_3(T)

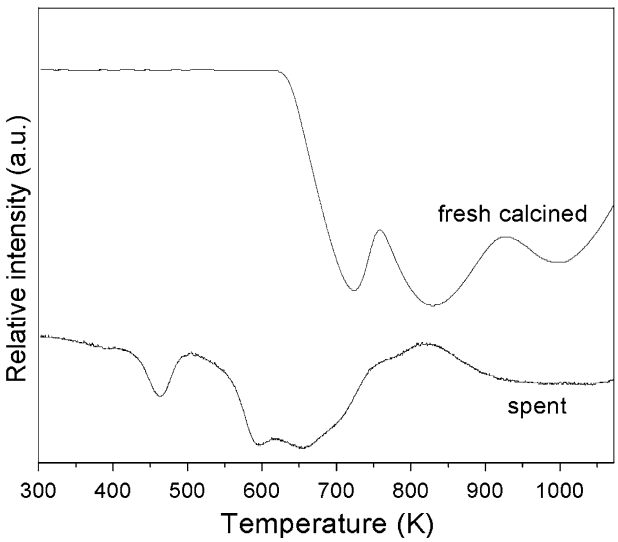

Fig. 6 H_2-TPR profiles of fresh calcined and spent 48 wt% Ni/Al_2O_3(T) catalysts

4 Conclusions

Two-step impregnations were found to yield catalysts with higher Ni dispersions compared to single impregnations, thus probably lead to smaller metal particle size and stronger interaction between metal species and support. Significantly higher hydrogen yields were observed over catalysts with high Ni content prepared by two-step impregnations such as 36 wt% Ni/Al_2O_3(T) and 48 wt% Ni/Al_2O_3(T) as compared to the corresponding catalysts prepared by single impregnations, whereas lower hydrogen yield was obtained over catalysts with low Ni content prepared by two-step impregnations such as 27 wt% Ni/Al_2O_3(T).

Acknowledgments We thank Prof. Hengyong Xu and Mr. Xiangang Ma for their help with HPLC analysis. We also thank Mr. Yingchong Ma and Ms. Yang Yang for their help with TOC analysis.

References

1. Ni M, Leung DYC, Leung MKH, Sumathy K (2006) Fuel Proc Technol 87:461
2. Cortright RD, Davda RR, Dumesic JA (2002) Nature 418:964
3. Davda RR, Dumesic JA (2004) Chem Commun 36
4. Tanksale A, Wong Y, Beltramini JN, Lu GQ (2007) Int J Hydrogen Energ 32:717
5. Xu YP, Tian ZJ, Wen GD, Xu ZS, Qu W, Lin LW (2006) Chem Lett 35:216
6. Valenzuela MB, Jones CW, Agrawal PK (2006) Energy Fuel 20:1744
7. Davda RR, Shabaker JW, Huber GW, Cortright RD, Dumesic JA (2005) Appl Catal B: Environ 56:171
8. Davda RR, Shabaker JW, Huber GW, Cortright RD, Dumesic JA (2003) Appl Catal B: Environ 43:13
9. Shabaker JW, Huber GW, Dumesic JA (2004) J Catal 222:180
10. Iriondo A, Barrio VL, Cambra JF, Arias PL, Güemez MB, Navarro RM, Sánchez- Sánchez MC, Fierro JLG (2008) Top Catal 49:46
11. Huber GW, Shabaker JW, Dumesic JA (2003) Science 300:2075
12. Shabaker JW, Huber GW, Dumesic JA (2004) J Catal 222:180
13. Wen GD, Xu YP, Ma HJ, Xu ZS, Tian ZJ (2008) Int J Hydrogen Energ 33:6657
14. Vos B, Poels E, Bliek A (2001) J Catal 198:77
15. Zhu XL, Huo PP, Zhang YP, Cheng DG, Liu CJ (2008) Appl Catal B: Environ 81:132
16. Zhang J, Xu HY, Jin XL, Ge QJ, Li WZ (2005) Appl Catal A: Gen 290:87
17. Alberton AL, Souza MMVM, Schmal M (2007) Catal Today 123:257
18. Bartholomew CH, Pannell RB (1980) J Catal 65:390
19. Mustard DG, Bartholomew CH (1981) J Catal 67:186
20. Lehnert K, Claus P (2008) Catal Commun 9:2543
21. Wang ZX, Pan Y, Dong T, Zhu XF, Kan T, Yuan LX, Torimoto Y, Sadakata M, Li QX (2007) Appl Catal A: Gen 320:24
22. Minowa T, Fang Z, Ogi T, Várhegyi G (1998) J Chem Eng Jpn 31:131
23. Kunkes EL, Simonetti DA, West RM, Serrano-Ruiz JC, Gärtner CA, Dumesic JA (2008) Science 322:417